BBA - Biomembranes 1861 (2019) 1388–1396

Contents lists available at ScienceDirect

BBA - Biomembranes

journal homepage: www.elsevier.com/locate/bbamem

Osmoprotective effect of ubiquinone in lipid vesicles modelling the *E. coli* plasma membrane

Emma K. Eriksson, Katarina Edwards, Philipp Grad, Lars Gedda, Víctor Agmo Hernández*

Department of Chemistry-BMC, Uppsala University, Box 576, SE-75123 Uppsala, Sweden

ARTICLE INFO

Keywords:
Liposomes
Water permeability
Membrane elasticity
Solanesol
Osmotic stress
Coenzyme Q10

ABSTRACT

Bacteria need to be able to adapt to sudden changes in their environment, including drastic changes in the surrounding osmolarity. As part of this adaptation, the cells adjust the composition of their cytoplasmic membrane. Recent studies have shown that ubiquinones, lipid soluble molecules involved in cell respiration, are overproduced by bacteria grown in hyperosmotic conditions and it is thus believed that these molecules can provide with osmoprotection. Hereby we explore the mechanisms behind these observations. Liposomes with a lipid headgroup composition mimicking that of the cytoplasmic membrane of *E. coli* are used as suitable models. The effect of ubiquinone-10 (Q10) on water transport across the membranes is characterized using a custom developed fluorescence-based experimental approach to simultaneously determine the membrane permeability coefficient and estimate the elastic resistance of the membrane towards deformation. It is shown that both parameters are affected by the presence of ubiquinone-10. Solanesol, a molecule similar to Q10 but lacking the quinone headgroup, also provides with osmoprotection although it only improves the resistance of the membrane against deformation. The fluorescence experiments are complemented by cryogenic transmission electron microscopy studies showing that the *E. coli* membrane mimics tend to flatten into spheroid oblate structures when osmotically stressed, suggesting the possibility of lipid segregation. In agreement with its proposed osmoprotective role, the flattening process is hindered by the presence of Q10.

1. Introduction

Bacteria typically stand in direct contact with their aqueous environment and, since the membranes enveloping the cells are water permeable, osmotic strains arising from changes in the concentration of solutes in the surrounding environment may alter the turgor pressure and prove fatal to the cells. Bacteria are therefore well-adapted to deal with drastic changes in extracellular osmolarities, usually by rapidly regulating the concentration of intracellular solutes, such as potassium glutamate, proline, glycine and trehalose [1–8], via enhanced endogenous synthesis or by triggering influx and efflux processes to transport solutes across the membrane. Bacteria can also modify the composition and properties of their cytoplasmic membranes when subjected to osmotic stress. In line with this, increased levels of, e.g., cardiolipin [9–12] have been observed in bacteria grown under hyperosmotic conditions. Recent findings indicate that the osmoprotection strategies used by bacteria also include some less expected modifications of the lipid content in the membranes.

Thus, a previous report by Sevin and Sauer [13] disclosed the somewhat surprising finding that the metabolic adaption of *E. coli* to sustained hyperosmotic salt stress includes a substantial increase in biosynthesis and membrane accumulation of the prenol lipid ubiquinone-8 (Q8). The accumulation of ubiquinone renders the bacteria more resistant to both sustained salt-induced osmotic stress and hyperosmotic salt shock. These rather unexpected observations have triggered new studies concerning the role that lipid soluble quinones may play as osmoprotectants in different kinds of cells [14] and led to suggestions of a possible membrane stabilizing role of ubiquinones

Abbreviations: BM, bacterial membrane (lipid composition POPE: *E. coli* PG: *E. coli* CL 75:19:6 molar ratio); BMM, bacterial membrane model (lipid composition POPE: POPG: CL from bovine heart 75:19:6 molar ratio); CF, 5(6)-carboxyfluorescein; CFA, cyclopropane fatty acid; CL, cardiolipin; Cryo-TEM, Cryogenic transmission electron microscopy; DPH, 1,6-diphenyl-1,3,5-hexatriene; IMM, Inner mitochondrial membrane; PBS, Phosphate buffered saline; PE, Phosphatidylethanolamine; PG, Phosphatidylglycerol; POPC, 1-palmitoyl-2-oleyl-sn-glycero-phosphocholine; POPE, 1-palmitoyl-2-oleoyl-sn-glycero-3-phosphoethanolamine; POPG, 1-palmitoyl-2-oleoyl-sn-glycero-3-phospho-(1'rac-glycerol); Q8, Ubiquinone-8; Q10, Ubiquinone-10

* Corresponding author.
E-mail addresses: emma.eriksson@kemi.uu.se (E.K. Eriksson), katarina.edwards@kemi.uu.se (K. Edwards), philipp.grad@kemi.uu.se (P. Grad), lars.gedda@kemi.uu.se (L. Gedda), victor.agmo@kemi.uu.se (V. Agmo Hernández).

https://doi.org/10.1016/j.bbamem.2019.04.008
Received 23 February 2018; Received in revised form 20 December 2018; Accepted 6 January 2019
Available online 23 April 2019

[15]. If proven correct, this stabilizing function could serve as an important complement to the well-established roles of ubiquinones in cellular respiration and as powerful lipid soluble antioxidants [16].

Although the mechanisms by which ubiquinones provide with osmoprotection have not yet been thoroughly investigated, it is likely that the observed protective effects are linked to an ability of the molecules to help regulate the water flow across the membrane. In the absence of proteins, and in accordance with a number of molecular dynamics simulations [17–19], the transport of water through lipid membranes proceeds via the partition of water into the membrane followed by its diffusion through the hydrophobic core. It could therefore be speculated that ubiquinones modify the way water interacts with and/or diffuses through the membrane. Previous studies [20,21] have documented the ability of Q10, the ubiquinone variant predominant in humans, to modify the intrinsic properties of lipid membranes. Hence, it has been shown that Q10 increases the lipid packing order, density and general stability of the membranes. As a consequence, Q10 modulates the membranes permeability towards small solutes, and enhances their resistance towards detergent action [20,21]. It is possible that a further consequence of this stabilization is the osmoprotective effect described above.

Indeed, results reported in the study by Sevin and Sauer [13] suggest that artificial phospholipid liposomes can be protected against collapse due to high osmotic stress by inclusion of 5 mol% Q10 in their membranes. It was proposed that ubiquinones and other isoprenoids (e.g., lycopene and solanesol) protected the liposomes against osmotic stress by increasing the hydrophobic thickness and the mechanical stability of the membrane. However, although the liposomes used in these investigations were built from biologically relevant lipids, the lipid composition did not reflect that of native *E. coli* membranes. Noteworthy, the liposomes contained an uncharacteristically low proportion of phosphatidylethanolamine (PE), and were devoid of the anionic lipid species phosphatidylglycerol (PG) and cardiolipin (CL). Both PE and CL are well known for their ability to promote the formation of non-bilayer assemblies, such as hexagonal (H_{II}) phase structures [22–24]. Alterations in lipid spontaneous curvature, as well as in electrostatics, can be expected to influence both permeability and micromechanical properties of the lipid membrane.

In order to identify the mechanisms giving origin to the osmoprotective effect of ubiquinones, we have in the present study carried out investigations based on the use of *E. coli*-relevant model membranes in combination with a customized fluorescence-based approach. More specifically, we have studied how liposomes with lipid composition mimicking that of the *E. coli* cytoplasmic membrane respond to salt-induced osmotic stress, and investigated how the response is affected by the presence of ubiquinones. The cytoplasmic membrane of *E. coli* was chosen as the modelled barrier since ubiquinone accumulation is expected to occur in this membrane. Furthermore, the outer membrane of *E. coli* is usually permeable to chloride and other solutes, and, therefore, irrelevant for salt-induced osmotic water transport [25].

In this report, we characterize the effect of ubiquinone according to two quantitative parameters: the osmosis-induced water permeability coefficient P_f, and the final relative liposome volume after the osmotic shock, which can be related to the membrane elastic resistance towards deformation. Both parameters were determined via carefully designed fluorescence quenching experiments. To complement these measurements, fluorescence anisotropy determinations were carried out in order to determine whether changes in the response to osmotic shock are related to changes in the lipid packing order. The results are moreover compared to those obtained by replacing ubiquinone with solanesol, a molecule very similar to ubiquinone, with a hydrophobic chain consisting of 9 isoprene units and a hydroxyl group replacing the quinone headgroup.

2. Materials and methods

2.1. Chemicals

Cardiolipin (CL) sodium salt from bovine heart, ubiquinone-8 (Q8), 1-palmitoyl-2-oleoyl-sn-glycero-3-phosphoethanolamine (POPE), 1-palmitoyl-2-oleoyl-sn-glycero-3-phospho-(1'rac-glycerol) (POPG) sodium salt, cardiolipin (*E. coli*) sodium salt, and L-α-phosphatidylglycerol (*E. coli*) sodium salt were bought from Avanti Polar Lipids (Alabaster, USA). 1-palmitoyl-2-oleyl-sn-glycero-phosphocholine (POPC) was obtained as a kind gift from Lipoid GmbH (Ludwigshafen, Germany). Ubiquinone-10 (Q10), solanesol (from tobacco leaves), cholesterol, polyethylene glycol *tert*-octylphenyl ether (Triton X-100), 5(6)-carboxyfluorescein (CF), 1,6-diphenyl-1,3,5-hexatriene (DPH), ammonium molybdate ($(NH_4)_6Mo_7O_{24}{\cdot}4H_2O$), sulfuric acid, methanol (Chromasolv® for HPLC, ≥ 99.9%), and 4-(2-hydroxyethyl)-1-piperazineethanesulfonic acid (Hepes) were purchased from Sigma-Aldrich (Steinheim, Germany). Chloroform (pro analysis), acetone, potassium antimony tartrate hemihydrate ($K(SbO)C_4H_4O_6{\cdot}0.5H_2O$) and L(+)-ascorbic acid were products from MERCK (Darmstadt, Germany). Hexane (mixed isomers) was from Acros Organics (Geel, Belgium). 99.7% spectroscopic grade ethanol was from Solveco (Rosersberg, Sweden). For all experiments, a phosphate buffered saline (PBS, 10 mM phosphate, 150 mM NaCl, pH = 7.4) was used unless indicated otherwise. All aqueous solutions were prepared using deionized water (18.2 MΩ cm) obtained from a Milli-Q system (Millipore, Bedford, USA). Experiments were performed at 25 °C unless otherwise indicated.

2.2. Preparation of liposomes

The lipids (including ubiquinones and solanesol) were either weighed or pipetted from stock solutions in chloroform to achieve the desired molar compositions. The lipids were further dissolved/diluted with ~2 mL chloroform, and the solvent was then let to evaporate under a gentle nitrogen stream. Any remaining traces of the solvent were removed under a vacuum (Squaroid vacuum oven, Lab Instruments, IL, USA) overnight. The lipid film was suspended in the desired aqueous solution and subjected to 5 freeze-thaw cycles (freezing with liquid nitrogen, thawing with a water bath at 60 °C). Mixtures containing CL (either bovine or from *E. coli*) were subjected instead to 15 freeze-thaw cycles to ensure mixing. The suspensions were thereafter extruded 31 times through a 100 nm pore size filter (Whatman plc, Kent, UK) using a Lipofast extruder (Avestin, Ottawa, Canada). Lipid mixtures containing POPE and/or ubiquinone-10 were pre-extruded 15 times through a 200 nm filter before the final 100 nm extrusion. POPC liposomes were extruded at room temperature. All other liposomes were extruded at 40 °C. After preparation, the suspensions were stored for 24 h in room temperature before starting the experiment to ensure reproducibility in the experiments [26].

The size distribution of the samples was obtained with the help of a NICOMP 380 particle sizer (Particle Sizing Systems, Port Richey, FL, US).

2.3. Determination of lipid:Q10 ratios

The effective lipid:Q10 ratios in the prepared liposomes were determined by independent estimations of the phosphorus and the Q10 content in the samples. Liposomes were prepared as described above, using Hepes buffered saline (HBS, 10 mM Hepes, 150 mM NaCl, pH = 7.4) instead of PBS. For the phosphorus analyses, three aliquots per sample were collected and treated according to the protocol described by Paraskova et al. [27]. Briefly, the samples were calcinated at 550 °C for at least 4 h and the obtained ashes were dissolved in 4 mL water. A volume of 1 mL of a freshly prepared mixture of seven parts of 1:3:10 $K(SbO)C_4H_4O_6{\cdot}0.5H_2O$ (2.75 mg mL^{-1}): $(NH_4)_6Mo_7O_{24}{\cdot}4H_2O$

(4% w/v): H_2SO_4 (2.5 M) and three parts of an ascorbic acid solution (0.1 M in water) were then added. After 15 min, the absorbance at 882 nm of the obtained solution was measured with an UV–Vis spectrometer (HP 8453, Agilent Technologies, Santa Clara, CA, USA). The concentration of phosphorus was calculated with the help of a standard curve prepared from different volumes of a phosphorus standard solution (0.65 mM, Sigma Aldrich, St. Louis, MO, USA). The concentration of phosphorus was related to that of the lipids considering that all lipids contain one phosphorus atom, save cardiolipin, which contains two.

The Q10 content was determined from three aliquots of different volumes taken from the same samples and treated as described by Kröger [28]. Briefly, a volume of 0.32 mL hexane (mixed isomers) and 0.48 mL methanol was added and the samples were vortexed for 1 min. A volume of 0.32 mL acetone was then added, followed by vortexing for 1 min and shaking for ~20 min. The sample was then centrifuged at 1500 ×*g* for 2 min. The upper phase was collected in a glass vial. The hexane extraction was then repeated with the aqueous phase. The hexane fractions were then pooled together and the solvent was then removed under a nitrogen flow followed by incubation in a vacuum for ~2 h. Finally, 2.5 mL spectroscopic grade ethanol was added and the absorbance at 275 nm was determined. The concentration of Q10 in the sample was calculated from its molar extinction coefficient in ethanol (12.6 $mM^{-1}\,cm^{-1}$) [28].

2.4. Fluorescence measurements

All fluorescence measurements were performed using a SPEX fluorolog 1650 0.2 m double spectrometer (SPEX industries, Edison, USA) in the right angle mode. Details for specific experiments are given below.

2.4.1. Fluorescence anisotropy

The steady-state fluorescence anisotropy of DPH incorporated into the lipid membrane was determined and related to the degree of membrane order in the hydrophobic region close to the polar headgroups [29]. The probe was added to the freshly prepared liposome samples from a concentrated stock solution (0.91 mM) in methanol. The probe:lipid ratio was 1:1000. The samples were incubated for at least 12 h in the dark before use in order to assure complete incorporation of the probe into the lipid membrane. The fluorescence spectrometer was equipped with two polarization filters, polarizing the excitation and the emission beams respectively. The excitation wavelength was set to 357 nm and the emission wavelength was set to 424 nm. The fluorescence intensity at all four possible combinations of the polarizing filters was then measured. The fluorescence anisotropy $< r >$ was calculated by:

$$< r > = \frac{I_{VV} - GI_{VH}}{I_{VV} + 2GI_{VH}} \quad (1)$$

where the grating factor $G = I_{HV}/I_{HH}$ is an instrumental correction factor. I_{XY} are the fluorescence intensities measured with the different combinations of the polarizers (X = excitation, Y = emission, H = horizontal, V = vertical). The experiments were performed at least in triplicates with each repetition being performed with a separate liposome batch. The error margins reported correspond to the standard error of all repetitions.

2.4.2. Water flow studies

The osmotic water permeability coefficient (P_f) was determined by monitoring the self-quenching of CF encapsulated in the liposomes in a way similar to what has been described previously [30,31]. Liposomes were prepared in a saline 15 mM CF solution isotonic with PBS (calculated osmolarity = 320 OsmM, pH = 7.4). Experimental determinations of the osmolarity of the buffer and of the used hypertonic solutions (see below) showed no significant deviations (< 5%) from the calculated values. After 24 h maturation time, the liposomes were separated from the non-encapsulated CF using a PD-10 gel filtration column (GE-Healthcare, Uppsala, Sweden) equilibrated with PBS. The collected liposomes were then diluted with PBS to a lipid concentration of 160 μM. For water flow determinations, the liposomes were subjected to a sudden increase in outer osmolarity by mixing 1:1 with hypertonic solutions with 12 different concentrations (varying between 25 and 500 mM excess NaCl) using a stopped flow apparatus (SFA-II Rapid Kinetics Accessory, TgK Scientific, England). The outward flow of water causes a decrease in the liposome volume and an increase in the inner CF concentration, resulting in a measurable decrease in fluorescence intensity. For most hypertonic solutions employed, only the fluorescence intensity at equilibrium was determined. For the solutions with 100, 250 and 500 mM excess NaCl, time-resolved measurements with a time resolution of 1 ms were performed in triplicates. At regular intervals (every 3–4 experiments), stock liposomes were mixed with PBS and the fluorescence intensity was recorded to account for changes in the free CF concentration. Finally, stock liposomes were mixed 1:1 with a 9.5 mM solution of Triton X-100 to induce complete release of the encapsulated CF. The obtained values were used to normalize the fluorescence intensities obtained in all experiments.

To account for stress-induced leakage of encapsulated CF, the experiments were repeated with liposomes filled with a completely quenched (100 mM) CF solution isotonic with PBS. Changes in fluorescence in these experiments were assumed to arise from leakage only. The fraction f of leaked CF was calculated from:

$$f = \frac{I_{(2)} - I_{(1)}}{I_{max} - I_{(1)}} \quad (2)$$

where $I_{(2)}$ is the fluorescence intensity upon mixing the liposomes with the hypertonic solutions, $I_{(1)}$ is the intensity when mixing with isotonic PBS, and I_{max} is the intensity at complete leakage from the liposomes (after mixing with Triton X-100).

In order to find the dependence of the normalized fluorescence intensities on the encapsulated CF concentration, calibration curves were built by preparing liposomes with all the studied compositions and filled with CF solutions with concentrations ranging from 10 mM to 100 mM. The fluorescence due to encapsulated CF was recorded immediately after separation from the non-encapsulated CF. The data was normalized against the fluorescence upon liposome solubilization with Triton X-100. The concentration of liposomes for each experiment was selected to keep the latter fluorescence in the linear range of the fluorescence vs. CF concentration curve.

The permeability coefficient of the liposomes was estimated from the time-resolved experiments and the permeability equation:

$$\frac{dX(t)}{dt} = -\frac{P_f V_w (SAV)}{RT}(\Delta P_{osmotic} - \Delta P_{elastic}) \quad (3)$$

where $X(t)$ is the relative volume (with respect to the initial volume) as a function of time, V_w is the molar volume of water ($1.8 \times 10^{-5}\,m^3\,mol^{-1}$), SAV is the initial liposome surface area to volume ratio (determined by DLS), $\Delta P_{osmotic} = RT(OsC_{out} - OsC_{in(0)}/X(t))$ is the osmotic pressure difference across the membrane, with OsC_{out} and $OsC_{in(0)}$ being the initial outer and inner osmolarities, respectively, and $\Delta P_{elastic}$ is the elastic pressure exerted by the liposome membrane upon deformation and which may oppose liposome shrinking. This pressure is dependent on the degree of deformation and the elastic properties of the membrane. The fact that the liposomes may present resistance towards deformation is usually not considered when studying the membrane osmotic permeability. In previous studies, it has commonly been assumed that the final relative liposome volume after the osmotic shock ($X(\infty)$) is known and equal to ($OsC_{in(0)}/OsC_{out}$), i.e., it has been assumed that the liposome does not present any resistance against deformation. In these cases, the estimated value of $X(\infty)$ at different levels of stress has been used to establish a relationship (sometimes assumed linear) between fluorescence intensity and relative volume X (e.g., [31,32]). Although for soft liposome membranes (e.g.,

liposomes composed of unsaturated lipids) the elastic resistance may be negligible, the same may not be true for more rigid membranes (e.g., membranes in the liquid ordered or gel phase states) or for liposome membranes already subjected to large elastic stress (e.g. for small unilamellar vesicles). In this report, we propose a new way of relating fluorescence intensity to liposomes volume without the need of assuming that the final conditions are known. The model considers the contribution of the encapsulated and the leaked CF to the total fluorescence intensity. Also, it takes into account that the inner concentration is affected not only by the transport of water, but also by the leakage of CF itself. Finally, as mentioned above, a careful calibration of the encapsulated CF relative fluorescence intensity (x_{CF}, normalized against the fluorescence intensity upon solubilization with Triton X-100) as a function of concentration was performed for all liposome compositions studied. Different stock solutions of CF were used in different preparations to account for variability between batches. The latter proved to have a more marked effect on the calibration curves than the liposome composition, likely due to minor variations in pH resulting in changes in the CF fluorescence intensity. However, the obtained curves overlap when normalized against the relative fluorescence observed at an encapsulated CF concentration of 15 mM. Therefore, a single calibration curve for all liposome samples and CF stock solutions tested could be obtained and fitted to a single exponential equation (Fig. S1 in the Supplementary Material) described by the initial value $y_N = 0.10 \pm 0.02$ the pre-exponential factor $A_N = 2.93 \pm 0.26$ and the decay constant $\tau_1 = 12.35 \pm 0.87$ mM.

During the osmosis-induced shrinkage experiments it is expected that the ionic strength of the inner solution will increase. Therefore, the fluorescence dependence on the ionic strength was characterized separately. No significant effect was observed in the range expected from the experiments.

From all these considerations, the following relationship between relative fluorescence and relative volume was established (see Section 2 in the Supplementary Material for details):

$$X(t) = \frac{(f(t)-1)[\mathrm{CF}]_{\mathrm{lip}(0)}(1-Z)}{\tau_1 \ln\left[\frac{1}{A_1}(x_{\mathrm{CF}}(t) - y_0 - f(t) + (f(t)-1)Z)\right]} \quad (4)$$

where $f(t)$ is the time dependent fraction of leaked CF, $[\mathrm{CF}]_{\mathrm{lip}(0)} = 15$ mM is the concentration of the CF solution used for liposome preparation, and y_0, A_1, and τ_1 are parameters describing the exponential relationship between relative fluorescence and encapsulated CF concentration. The values of y_0 and A_1 are calculated for each sample from the calibration parameters y_N and A_N and the relative fluorescence obtained for the sample directly after separation from free CF. Finally, Z is a parameter accounting for changes in the initial encapsulated and free CF concentrations due to spontaneous leakage occurred between the time of separation and the start of the water transport experiment, and is given by:

$$Z = \frac{\tau_1(x_1 - x_{\mathrm{lip}([\mathrm{CF}]_{\mathrm{lip}(0)})})}{\tau_1 + [\mathrm{CF}]_{\mathrm{lip}(0)}(x_{\mathrm{lip}([\mathrm{CF}]_{\mathrm{lip}(0)})} - y_0)} \quad (5)$$

where $x_{\mathrm{lip}([\mathrm{CF}]_{\mathrm{lip}(0)})}$ is the relative fluorescence immediately after separation (before any spontaneous leakage has occurred) and x_1 is the relative fluorescence right before the water transport experiment.

At equilibrium, the rate of volume change should be zero and, therefore, at equilibrium conditions, $\Delta P_{\mathrm{elastic}} = \Delta P_{\mathrm{osmotic}} = RT(\mathrm{Os}C_{\mathrm{out}} - \mathrm{Os}C_{\mathrm{in}(0)}/X(\infty))$. By performing experiments where the liposomes are subjected to different outer osmolarities, the dependence of $\Delta P_{\mathrm{elastic}}$ on the relative volume X could be established experimentally for each individual sample. However, no universal (valid for all samples studied) relationship between $\Delta P_{\mathrm{elastic}}$ and X could be identified. Therefore, the relationship between the parameters was modelled as linear between each of the experimental points, with the slope and y-intercept varying according to the values of X. The permeability equation was thus rewritten to:

$$\frac{dX(t)}{dt} = X'(t) = -P_f V_w (SAV)\left(\mathrm{Os}C_{\mathrm{out}} - \frac{\mathrm{Os}C_{\mathrm{in}(0)}}{X(t)} - (m_X X(t) + b_X)\right) \quad (6)$$

where m_x and b_x are the slope and y-intercept values determined for each sample and which vary depending on the value of $X(t)$. Note that this term corrects also for potential changes in the osmotic pressure difference due to changes in the activity coefficients of the solutes upon liposome shrinking.

To determine P_f, the experimentally determined $X(t)$ vs. t curves were fitted to a single exponential equation ($X(t) = a_0 + A * \exp.(-k * t)$, where $a_0 = X(\infty)$). For every single experimental point, a value of $X'(t) / P_f$ was calculated according to Eq. 6. The obtained curve was fitted to an equation of the form $X'(t)/P_f = -A_2 * \exp.(-k * t)$. The value of P_f can thus be calculated from the two fitting curves as:

$$P_f = \frac{k \times A}{A_2} \quad (7)$$

All determinations of P_f were carried out at three different levels of hyperosmotic stress (excess outer NaCl concentration: 50 mM, 125 mM and 250 mM), with triplicates for each level. For *E. coli* model membranes, the experiments were repeated with different liposome batches to ensure reproducibility.

The ability of our experimental approach and equations to relate fluorescence measurements to relative liposome volume was tested by studying the response of POPC and POPC:cholesterol (3:2) liposomes to osmotic stress (see Section 3 in the Supplementary Material). The permeability coefficient values determined for these systems ($(2.40 \pm 0.28) \times 10^{-3}$ cm s^{-1}and $(0.653 \pm 0.03) \times 10^{-3}$ cm s^{-1} for POPC and POPC:cholesterol liposomes, respectively), are in agreement with the P_f values obtained for liposomes of similar composition by Rawicz et al. [33] using micropipette aspiration ($P_f = (3.40 \pm 0.7) \times 10^{-3}$ cm s^{-1} for steareoyl oleoyl phosphocholine, SOPC, at 30 °C; and $P_f = (0.640 \pm 0.13) \times 10^{-3}$ cm s^{-1} for SOPC:cholesterol 1:1 at 30 °C), supporting the validity of the proposed method. Furthermore, the values of $X(\infty)$ (see Table S1 in the Supplementary Material) obtained at different levels of osmotic stress agree with the known elastic properties of the liposomes used.

2.5. Cryo-TEM

Samples were analysed by cryogenic transmission electron microscopy (cryo-TEM) following the description by Almgren et al. [34]. To perform the analyses, a sample drop was placed onto a copper grid, reinforced with a holey polymer film, under controlled temperature and humidity conditions. After blotting away excess liquid by use of a filter paper, the grid was plunged into liquid ethane to vitrify the sample films and thereafter transferred to the microscope. The sample was protected from atmospheric conditions and was kept below −160 °C during the transfer. Analyses were performed at cryogenic temperature with a Zeiss TEM Libra 120 instrument (Carl Zeiss AG, Oberkochen, Germany) operating in zero-loss bright-field mode. The digital images were recorded under low-dose conditions with a BioVision Pro-SM Slow Scan CCD camera (Proscan elektronische Systeme GmbH, Scheuring, Germany).

For cryo-TEM based quantitative descriptions of the samples, all observed particles were manually counted and classified as spherical unilamellar, bi- and multilamellar/multivesicular, or collapsed unilamellar vesicles. The latter were observed as oblate structures with orientations ranging from perpendicular to parallel with the incoming electron beam (Fig. S3 in the Supplementary Material). To ensure objectivity of the classification, the cryo-TEM particle classifications were done as blind studies, with the sample analysed being unknown to the operator. At least 180 particles were counted for each sample.

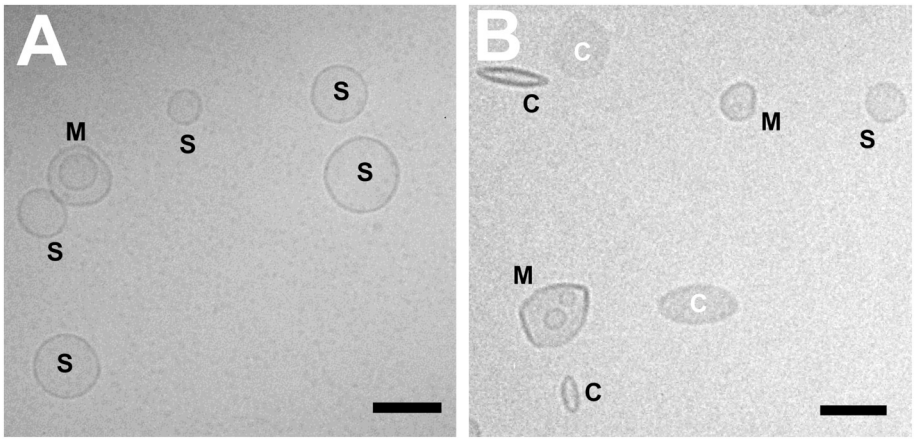

Fig. 1. Representative cryo-TEM pictures illustrating the appearance of the samples before (A) and after (B) osmotic shock. Images were obtained for A) BM:Q10 (1.6 mol% Q10) liposomes in an isotonic solution, and B) BM liposomes subjected to osmotic shock ($OsC_{in(0)}$ / OsC_{out} = 0.762). Bar: 100 nm. The labels denote the different structures observed: S: spherical unilamellar liposomes; M: Bi- or multilamellar/multivesicular liposomes, and C: collapsed unilamellar liposomes. The latter can be observed at different orientations. Top and sideway views are denoted with white and black labels, respectively. BM: Bacterial membrane (POPE: PG from *E. coli*: CL from *E. coli*, 75:19:6).

2.6. Statistical analysis

In order to test for significant differences, data were analysed by Welch's *t*-test. Significant differences were defined by $p < 0.05$.

3. Results

3.1. Verification of the osmoprotective effect

Before proceeding with more detailed characterizations, we found it important to confirm that the previously observed osmoprotective effects of ubiquinone persist when the liposome composition is adapted to resemble that of the *E. coli* plasma membrane. For these initial investigations liposomes were prepared from a lipid mixture (abbreviated BM: bacterial membrane) containing POPE, PG from *E. coli*, and CL from *E. coli* (75:19:6 molar ratio, mimicking the headgroup composition of cytoplasmic *E. coli* membranes reported by Morein et al. [35]). The described custom mixture was preferred over commercial *E. coli* polar lipid extracts given that the latter incorporates lipids from not only the cytoplasmic, but also the outer membrane of the bacteria. POPE was chosen over PE extracts from *E. coli* given that the latter consists, according to the provider, mainly of palmitoyl (33.6%) and oleoyl (34.1%) fatty acid substitutions, and is therefore roughly equivalent to POPE.

Cryo-TEM was employed to visualize the response of pure and ubiquinone (Q10 and Q8 variants) supplemented liposomes to an acute osmotic shock induced by addition of excess salt to the external buffer. As revealed by cryo-TEM (Fig. 1), the unstressed samples were dominated by unilamellar liposomes displaying a close to perfectly spherical shape. In addition to these, some distorted or flattened unilamellar liposomes were also observed. The samples contained moreover a small population of bi- and multilamellar/multivesicular structures. For all vesicles imaged in a sample, the proportion corresponding to each kind of structure was determined (Fig. 2). Upon addition of 50 mM excess salt, resulting in an initial inner/outer osmolarity ratio $OsC_{in(0)}$ / OsC_{out} = 0.762, the proportion of bi- and multilamellar/multivesicular structures remained virtually unchanged, but, importantly, the overall shape of the liposomes was notably affected. Thus, the number of flattened liposomes increased while the population of spherical liposomes decreased. These observations show that the liposomes react to the hyperosmotic stress by collapsing into flat, oblate spheroidal structures. As evident from a comparison of the data presented in Fig. 2, the presence of the ubiquinones clearly decreased the liposomes' tendency to deflate in response to the osmotic shock. Hence, for BM liposomes, the addition of salt causes a 65% drop in the proportion of spherical unilamellar liposomes. In the case of liposomes supplemented with Q10 or Q8 (25:1 mixing ratio) the addition of salt causes a corresponding drop of, respectively, 40% and 56%.

These observations suggest that both Q8 and Q10 indeed have an osmoprotective effect in liposomes with compositions resembling that of *E. coli* cytoplasmic membranes. However, the analysis of cryo-TEM images does not provide with any quantitative measurement of this effect.

3.2. Role of ubiquinone on the osmotic water transport across lipid membranes

The experiments were performed with liposomes based on the BM mixture as well as with liposomes composed of a mixture with the same relative headgroup composition but with better controlled fatty acid substitutions. This mixture is denoted BMM: bacterial membrane model, and consists of POPE (75 mol%), POPG (19 mol%) and bovine heart CL (6 mol%). Experiments were also performed with POPC-based liposomes, since the effect of Q10 on the properties of POPC membranes has been previously studied in detail [20].

3.2.1. Liposome characterization

Cryo-TEM investigations confirmed the formation of liposomes with the BM (Fig. 1A) and BMM compositions (Fig. 3A). As shown in Fig. 3B, the BMM liposomes responded to salt induced osmotic stress by flattening in a similar manner as observed for the BM composition

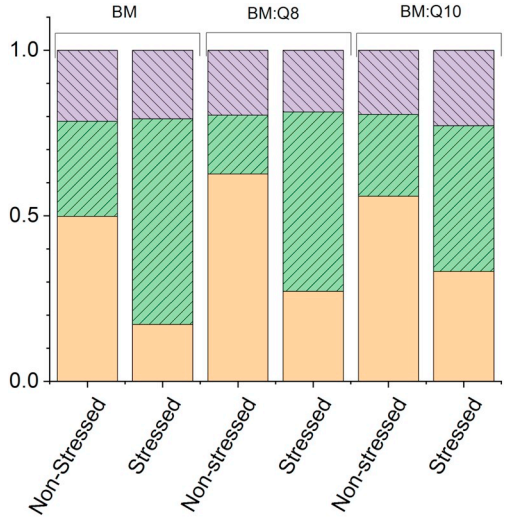

Fig. 2. Relative proportions of the different structures observed in the studied samples classified according to the criteria described in Fig. 1. Stressed liposomes were subjected to a ratio $OsC_{in(0)}$/OsC_{out} = 0.762. ▨: Bi- and multilamellar/multivesicular, ▨: Collapsed unilamellar, ▭: Spherical unilamellar. BM: Bacterial membrane (POPE: PG from *E. coli*: CL from *E. coli*, 75:19:6).

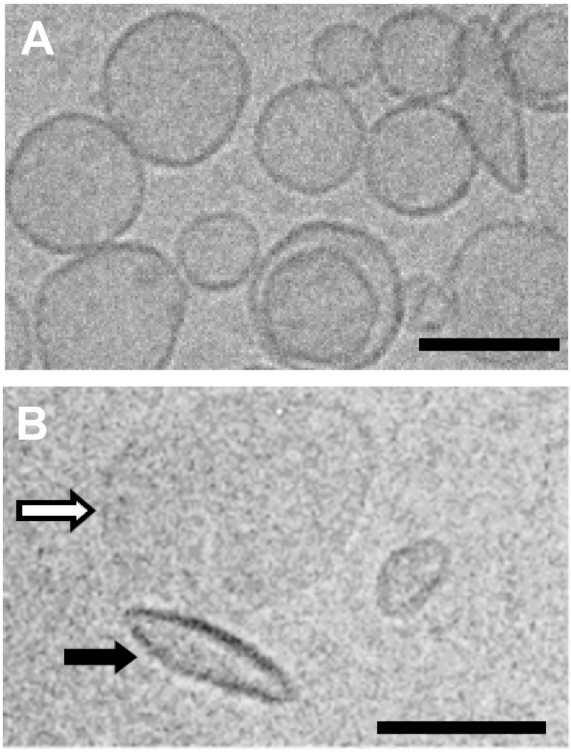

Fig. 3. Cryo-TEM images of BMM (POPE:POPG:CL 75:19:6) liposomes before (A) and after (B) been subjected to osmotic stress ($OsC_{in(0)}$ / OsC_{out} = 0.39). Upon osmotic shock, liposomes flatten to accommodate the excess area. Flattened structures are seen sideways (black arrow) or from the top (white arrow). Bars: 100 nm.

(Fig. 1B). The phase transition temperatures for the BM and BMM liposomes were determined to be ~18 °C and ~20.5 °C, respectively (Fig. S4 in the Supplementary Material). All experiments were thus carried out at 25 °C to ensure that the membranes were in the liquid crystalline phase state. When including Q10, the effective lipid:Q10 ratio, as determined by phosphorus and Q10 determinations (see experimental section), was 60:1 (~1.6 mol% Q10), for both the BM and BMM liposomes. The Q10 content in the membranes is therefore representative of the expected ubiquinone content in osmotically stressed *E. coli* [13]. The incorporation of Q10 into the bacterial membrane mimics is lower than what is achieved with POPC (3.3 mol%) [20] and inner mitochondria membrane (IMM) mimics (2.1 mol%) [21], and very similar to what is obtained in pure POPE liposomes (1.6 mol%) [21] at the same lipid:Q10 mixing ratio (25:1).

3.2.2. Effect of ubiquinone and solanesol on lipid packing order

Measurements of the fluorescence anisotropy $< r >$ (Fig. 4) revealed that BMM liposomes are more ordered than POPC membranes, but have a lower degree of order than the liposomes in which bacterial lipids have been used (BM). The higher order of the latter membranes may arise from the rather high content of cyclopropane fatty acid (CFA) substitutions in the bacterial lipids used (according to the provider, approximately 32 and 27 mol% CFA substitutions in the PG and CL samples, respectively). CFA substituted lipids are produced by different kinds of bacteria mainly in response to stress and extreme growth conditions, and they seem to be key in providing the membrane with protection against changes in the environment [36–38], including variations in pH, high hydrostatic pressure, and hyperosmotic conditions. These effects of CFA substituted lipids are likely to be coupled to an increased membrane order, in agreement with our results and with the conclusions from recently reported molecular dynamics studies [39].

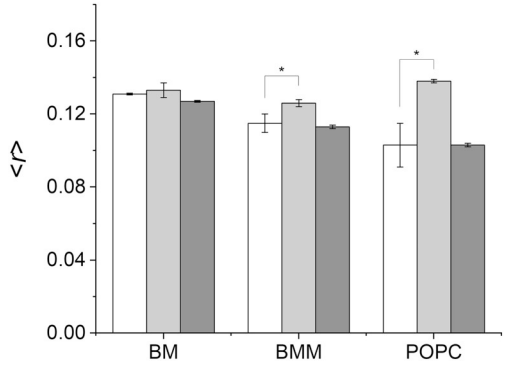

Fig. 4. Fluorescence anisotropy $< r >$ obtained for liposomes without (white bars) and with the incorporation of Q10 (light grey) or solanesol (dark grey). BM: Bacterial membrane (POPE:PG from *E. coli*:CL from *E. coli*, 75:19:6), BMM: bacterial membrane model (POPE:POPG:CL, 75:19:6). The lipid:Q10 and lipid:solanesol mixing ratio was 25:1 in all cases. Significant differences ($p < 0.05$) upon inclusion of Q10 or solanesol are indicated with an asterisk.

Inclusion of Q10 causes an increase in the value of $< r >$ for all studied liposome compositions (Fig. 4), indicating that the membranes become more ordered in all cases, although the effect on BM membranes is not statistically significant. BM liposomes supplemented with Q8 ($< r > = 0.130 \pm 0.004$) showed also no significant difference with the pure BM composition. It is also observed that solanesol does not significantly affect the fluorescence anisotropy of any of the samples.

3.2.3. Osmotic water permeability coefficient

Time-traces of the relative liposome volume ($V(t) / V_0 = X(t)$) were recorded for BM, BMM and POPC liposomes subjected to three different levels of osmotic stress. As illustrated for BM liposomes in Fig. 5, the relative liposome volume decreases rapidly upon osmotic shock until it reaches a constant value once equilibrium has been achieved. The obtained results were used to determine the values of P_f (related to the rate of decrease of the relative volume) and $X(\infty)$ (relative liposome volume at equilibrium) for each studied sample.

It is observed that the measured osmotic water permeability coefficient P_f values decrease for all kinds of liposomes (Fig. 6) upon inclusion of the ubiquinone. However, and in line with the fluorescence

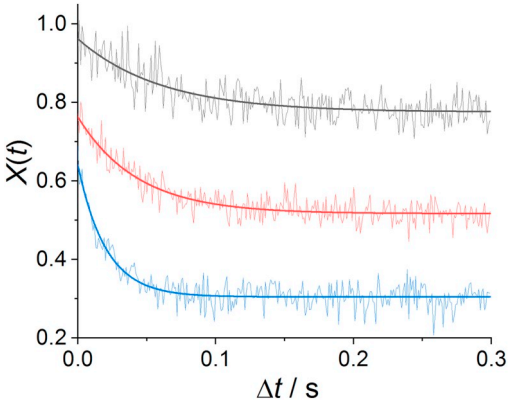

Fig. 5. Relative volume as a function of time $X(t)$ for BM liposomes (POPE: PG from *E. coli*: CL from *E. coli*, 75:19:6) subjected to hypertonic solutions with, respectively, 50 mM (black), 125 mM (red) and 250 mM (blue) excess NaCl (selected experiments). Thick solid lines represent the fitting to a single exponential equation. From these fittings, P_f and $X(\infty)$ values can be calculated according to the procedure described in the methods section. Δt in the *x*-axis indicates that the data is taken after a certain dead-time (< 8 ms) dependent on the mixing accessory employed. (For interpretation of the references to colour in this figure legend, the reader is referred to the web version of this article.)

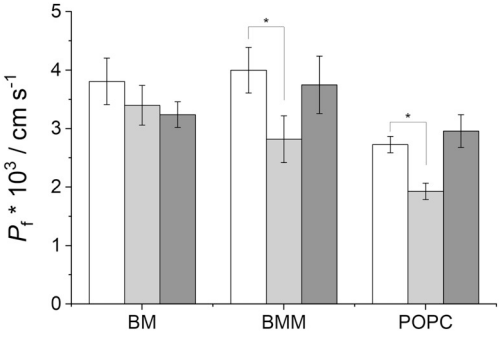

Fig. 6. Osmotic water permeability coefficient P_f values obtained for liposomes without (white bars) and with the incorporation of Q10 (light grey) or solanesol (dark grey). BM: Bacterial membrane (POPE:PG from *E. coli*:CL from *E. coli*, 75:19:6), BMM: bacterial membrane model (POPE:POPG:CL, 75:19:6). The lipid:Q10 and lipid:solanesol mixing ratio was 25:1 in all cases. The obtained P_f values were independent on the concentration of the hypertonic solutions for all the liposomes tested. Significant differences ($p < 0.05$) upon inclusion of Q10 or solanesol are indicated with an asterisk.

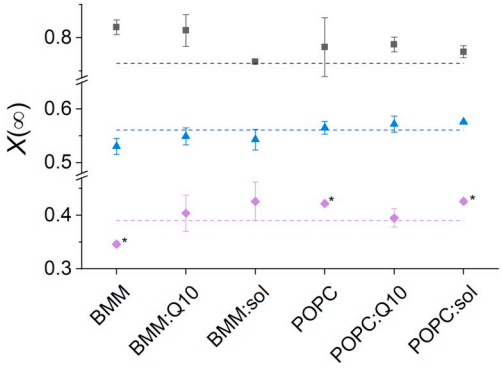

Fig. 7. Determined ratio between the final and the initial volumes ($X(\infty)$) upon osmosis-induced liposome shrinking at different levels of salt excess for POPC and BMM liposomes (POPE:POPG:CL 75:19:6) with and without the inclusion of Q10 or solanesol (25:1 lipid:Q10 and lipid:solanesol molar mixing ratios). The dashed horizontal lines represent the expected $X(\infty)$ values to achieve isoosmolarity. Significant deviations from these values are indicated with an asterisk. Three levels of NaCl excess are plotted: 50 mM excess (black squares), 125 mM excess (blue triangles), and 250 mM excess (purple circles). (For interpretation of the references to colour in this figure legend, the reader is referred to the web version of this article.)

anisotropy data, this decrease is not significant for the model using bacterial lipids (BM). For this latter case, the inclusion of Q8 has also no significant effect on the permeability coefficient ($P_f = (4.13 \pm 0.23) \times 10^{-3}$ cm s^{-1}). A similar phenomenon was observed in the previous report by Sevin and Sauer [13], where liposomes formed with a mixture of natural lipid extracts from *E. coli*, egg and soy were used and no osmoprotective effect of Q10 could be observed at a ubiquinone content of 1 w/w%, even though the same proportion seemed to effectively protect bacteria.

It is likely that the discrepancy between the results obtained with synthetic (POPC and BMM membranes) and natural (BM membrane and the liposomes used by Sevin and Sauer [13]) lipids can be attributed to the rather heterogeneous fatty acid distribution of natural lipid extracts. For membranes composed by natural lipids, the effect of variations in composition between liposomes may be larger than the effect of the inclusion of ubiquinone. More importantly, the heterogeneity in composition can also cause variations in the ubiquinone content of individual liposomes. In the present case, the cryo-TEM results indeed show that liposomes in the same sample may react differently to osmotic shock: some of them collapse, while some are protected, and this observation can be coupled to differences in the liposome's composition.

To diminish the possible effect of these variations, BMM-based liposomes, with better controlled fatty acid substitutions, where preferred for further analyses. Also, Q10 was preferred over Q8 given that the effect of Q10 on membranes rich in palmitoyl and oleoyl fatty acid substitutions is well-documented [20,21], and that the supplementation of Q10 has been shown to restore osmotolerance on *E. coli* mutants lacking Q8, indicating that Q8 and Q10 have equivalent osmoprotective effects in *E. coli* [13].

The effect of ubiquinone on the BMM liposomes becomes more evident when saturating the membranes with Q10 (lipid:Q10 mixing ratio 9:1). In this case, the permeability coefficient decreases to a value of $(1.62 \pm 0.23) \times 10^{-3}$ cm s^{-1}, less than half the P_f value determined for the unmodified membrane. Unfortunately, the presence of Q10-rich non-lamellar structures in this sample prevented an exact determination of the saturation conditions and the fluorescence anisotropy of the liposomes.

Concerning solanesol, it is observed (Fig. 6) that the molecule apparently increases the water permeability of POPC liposomes, while having the opposite effect on BM and BMM liposomes. However, the effect of the molecule was not significant for any of the samples tested. A preparation of solanesol-saturated BMM liposomes (mixing ratio 9:1) showed a slightly (not significantly) decreased permeability factor ($(3.47 \pm 1.88) \times 10^{-3}$ cm s^{-1}).

3.2.4. Relative liposome volume at equilibrium

Concerning the final relative volume at equilibrium $X(\infty)$, the inclusion of Q10 or solanesol does not affect the values of $X(\infty)$ for POPC membranes at any of the tested salt concentrations (Fig. 7). Furthermore, for these liposomes, $X(\infty)$ corresponds to the initial inner/outer ($OsC_{in(0)}/OsC_{out}$) osmolarity ratios when the excess salt concentration is 50 and 125 mM, implying that there is no elastic resistance preventing deformation of the liposomes (as expected for the very soft POPC membranes). The only values that appear larger than expected are obtained with the strongest osmotic stress (excess salt 250 mM), likely due to the accumulated elastic tension present at this point, which would prevent further deformation/shrinking of the liposome.

Remarkably, the results in Fig. 7 show that the pure BMM liposomes only present resistance towards deformation at low levels of osmotic stress (50 mM excess salt). For excess salt concentrations of 125 and 250 mM, the liposomes shrink beyond what is necessary to achieve isoosmolarity, suggesting that the elastic tension ***promotes*** deformation instead of preventing it. As illustrated in Figs. 1B and 3B, analysis by cryo-TEM has shown that, for the BM and BMM liposomes, the decrease in volume accompanying the osmotic shock results in flattening of the liposomes into oblate structures. This behavior is different from the inward deformations (invaginations) typically observed for liposomes built from non-charged lipids (see Wessman et al. [40] and Fig. S5 in the Supplementary Material). These invaginations can eventually lead to internal budding and the formation of bilamellar structures. The fact that no increase in the proportion of bi- and multi- lamellar structures is observed in stressed BM liposomes (Fig. 2) further suggest that these vesicles do not respond to osmotic stress by deforming inwards and that the formation of flattened structures is preferred. The oblate structures observed for BM and BMM have a highly curved equator and two rather planar membrane areas. The flattening process upon salt-induced osmotic stress may therefore involve segregation of the lipid components with the planar part of the flattened liposome being rich in POPE (which gives very compact and rigid membranes [21]) and the curved equator being rich in POPG and CL in the outer and inner lipid leaflets, respectively. It is in fact known that CL accumulates at the curved poles and folds of, respectively, bacterial cells and mitochondrial membranes [41], very likely because of its tendency to form structures with negative curvature [42,43]. In the current case, this tendency is enhanced by the increase in ionic strength, screening thus the repulsion between the CL headgroups. The proposed lipid segregation, would allow

accommodating the excess membrane area upon liposome shrinking without imposing excessive strain in the membrane. Indeed, the flattening of the rigid POPE-rich region and the segregation of CL to negative curvature areas (the inner leaflet of the curved equator) can be favorable to the deformation, resulting in the shrinking-promoting effect observed for BMM liposomes at high excess salt concentrations. Interestingly, the data in Fig. 7 suggests that this effect vanishes upon inclusion of Q10 or solanesol, meaning that both molecules can protect the BMM liposomes against the effect of salt-induced osmotic shock.

4. Discussion

Taken together, the results suggest that Q10 can provide with osmoprotection via different mechanisms depending on the composition of the membrane. For POPC membranes, it seems likely that the effect arises primarily from an increased degree of membrane order and more tightly packed lipids, and is thus correlated with other observed phenomena upon inclusion of Q10 in POPC membranes (e.g., decreased solute leakage rates) reported previously [20]. The obtained values of P_f correlate well with previously reported data on fluorescence anisotropy ($< r >$), rate of spontaneous CF leakage (k_L), and headgroup area (area/lipid) (Fig. 8).

As can be observed in the figure, a strong correlation exists between these variables. More condensed membranes (smaller area/lipid) are characterized by a higher lipid order (fluorescence anisotropy), lower CF leakage rate and lower water permeability. The observed clear correlation between area/lipid and water permeability is in agreement with a previous report by Mathai et al. [32]. It is to be noted that inclusion of solanesol in the POPC membrane does not significantly affect the permeability coefficient, or any of the other parameters, indicating that the quinone headgroup is important to provide with osmoprotecting capabilities.

In the case of BMM membranes, the difference in the effects noted for Q10 and solanesol on the lipid packing order (Fig. 4) can be explained by considering that at least a fraction of the Q10 likely is positioned with the quinone moiety close to the headgroup area in the membrane [21,46,47]. It is also worth mentioning that solanesol has

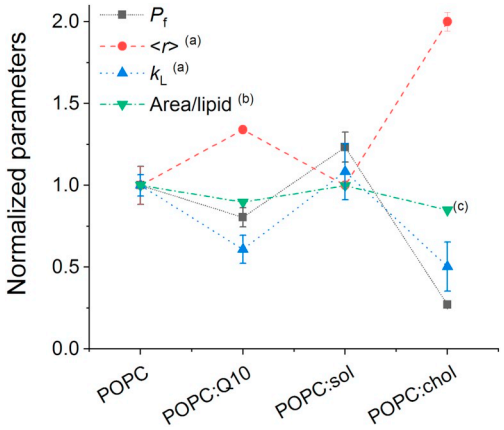

Fig. 8. Normalized parameters showing the relation between obtained permeability coefficient P_f, and reported fluorescence anisotropy $< r >$, rate constant of initial leakage k_L and area/lipid for POPC, POPC:Q10 (25:1), POPC:solanesol (25:1)* and POPC:cholesterol (3:2) liposomes. Compositions are given in molar mixing ratios. The values are normalized against the values obtained for POPC liposomes ($P_f = 2.40 \pm 0.28 / (10^{-3}\,\mathrm{cm\,s^{-1}})$), $< r > = 0.103 \pm 0.012$ (Agmo Hernández et al. [20]), $k_L = 4.65 \pm 0.3 / (10^{-4}\,\mathrm{s^{-1}})$ (Agmo Hernández et al. [20]) and Area/lipid = 68.3 / Å^2 (Kučerka et al. [44]). [(a)]Agmo Hernández et al. [20]. [(b)]Calculated from membrane density data reported by Agmo Hernández et al. [20] unless otherwise indicated. [(c)]Pan et al. [45]. *Spontaneous leakage rate and area/lipid for POPC:solanesol correspond to a 50:1 mixing ratio.

been shown to decrease the order in both pure POPE and pure CL membranes [21], presumably due to the enhanced negative curvature stress upon its inclusion. This effect is not observed in BMM membranes, even though CL and POPE form 81% of the total lipid content, suggesting that the proportion of POPG present is enough to disperse the negative curvature that is induced by solanesol.

As judged by the obtained permeability coefficients (Fig. 6), Q10 appears to have a similar effect in BMM and POPC membranes. On the other hand, the effect of Q10 on the fluorescence anisotropy was much more modest in BMM as compared to the POPC membranes. Furthermore, the BMM based liposomes displayed in general a higher P_f than POPC based liposomes, even though their fluorescence anisotropy values were higher. In other words, the higher water permeability for BMM as compared to POPC cannot be attributed to differences in membrane order. Osmosis-induced leakage of CF was negligible in all samples (< 0.05% of the encapsulated CF content in all experiments), discarding thus also the possibility that water is transported through large transient pores. Given that the thickness of the hydrophobic part of BMM and POPC membranes is rather similar, the enhanced permeability of BMM-based membranes must stem from the different headgroup composition. PE, PG and CL can form hydrogen bonds with water, both as donors and as receptors, and water adsorption onto and partition into the membrane can therefore be enhanced by high local surface concentrations. Enhanced adsorption and partition can be translated to faster transport across the membrane. Q10 is likely to slow down this process by condensing the membrane and increasing its packing order, making it thus more difficult for water to diffuse through.

Noteworthy, as revealed in Fig. 7, solanesol and Q10 seem to protect BMM membranes against excessive deformation. The osmoprotective effect of Q10 may therefore be traced back to two complementary mechanisms: an enhanced lipid packing order resulting in a decreased permeability coefficient; and an increased elastic stress-induced pressure providing with resistance against deformation, and therefore, decreasing the water flow. The latter effect is independent of the quinone moiety, as shown by the experiments performed with solanesol.

A plausible explanation for Q10's and solanesol's protective effect against deformation can be found by considering the possibility that the flattening of the liposomes is coupled to lipid segregation. The solubility of Q10 and solanesol has been shown to be very low in POPE membranes [21]. On the other hand, determinations of the Q10 content in liposomes made purely of CL showed that Q10 was incorporated at levels above 15 mol% and cryo-TEM experiments confirmed that, at these proportions, Q10 clearly enhances the negative curvature stress of the membrane (Fig. S6 in the Supplementary Material). Upon the proposed lipid segregation, it is therefore likely that Q10 would accumulate at the fluid CL-rich edges, increasing their packing order and preventing the liposomes from deforming further. Even more importantly, the elastic tension and the hydrophobic volume would be enhanced at these edges, preventing further flattening of the liposome and explaining why solanesol also has a protective effect.

5. Conclusions

Although the osmoprotective role of ubiquinone has been previously documented, the mechanisms behind it have so far remained unknown. The results in this report provide with a physicochemical explanation for the observed osmoprotective effect of ubiquinones, and two mechanisms are identified, one related to the quinone headgroup and one dependent exclusively on the hydrophobic polyisoprenoid chain. The headgroup-dependent effect is the reduction of the permeability coefficient of the membrane by increasing the packing order of the lipids. This effect is observed both in soft POPC membranes and in the more rigid BMM mimics. The polyisoprenoid dependent mechanism is the protection against deformation of the membrane, creating thus an elastic pressure that counteracts the osmotic driven water flow. This

mechanism is negligible for POPC liposomes, but it is of high relevance for the *E. coli* membrane models used, and can explain the osmoprotective effect of solanesol observed in experiments with *E. coli* [13].

Transparency document

The Transparency document associated with this article can be found, in online version.

Acknowledgements

KE gratefully acknowledges financial support from the Swedish Research Council (2016-03464) and the Swedish Cancer Society (17 0566). The authors thank León Zendejas Medina, Christian Hartman and Dr. Jonny Eriksson for assistance with the experimental work. The POPC material was a kind gift from Lipoid, Ludwigshafen, Germany.

Appendix A. Supplementary data

Supplementary data to this article can be found online at https://doi.org/10.1016/j.dummy.2019.01.002.

References

[1] W. Epstein, Osmoregulation by potassium transport in Escherichia coli, FEMS Microbiol. Lett. 39 (1986) 73–78.
[2] J.L. Milner, S. Grothe, J.M. Wood, Proline porter II is activated by a hyperosmotic shift in both whole cells and membrane vesicles of Escherichia coli K12, J. Biol. Chem. 263 (1988) 14900–14905.
[3] A.R. Strom, I. Kaasen, Trehalose metabolism in Escherichia coli: stress protection and stress regulation of gene expression, Mol. Microbiol. 8 (1993) 205–210.
[4] O.B. Styrvold, A.R. Strom, Synthesis, accumulation, and excretion of trehalose in osmotically stressed Escherichia coli K-12 strains: influence of amber suppressors and function of the periplasmic trehalase, J. Bacteriol. 173 (1991) 1187–1192.
[5] S.P. Koo, C.F. Higgins, I.R. Booth, Regulation of compatible solute accumulation in Salmonella typhimurium: evidence for a glycine betaine efflux system, J. Gen. Microbiol. 137 (1991) 2617–2625.
[6] M.T. Record Jr., E.S. Courtenay, D.S. Cayley, H.J. Guttman, Responses of E. coli to osmotic stress: large changes in amounts of cytoplasmic solutes and water, Trends Biochem. Sci. 23 (1998) 143–148.
[7] R. Krämer, Bacterial stimulus perception and signal transduction: response to osmotic stress, Chem. Rec. 10 (2010) 217–229.
[8] J.M. Wood, Bacterial responses to osmotic challenges, J. Gen. Physiol. 145 (2015) 381.
[9] T. Romantsov, Z. Guan, J.M. Wood, Cardiolipin and the osmotic stress responses of bacteria, Biochim. Biophys. Acta 1788 (2009) 2092–2100.
[10] M. Tsai, R.L. Ohniwa, Y. Kato, S.L. Takeshita, T. Ohta, S. Saito, H. Hayashi, K. Morikawa, Staphylococcus aureus requires cardiolipin for survival under conditions of high salinity, BMC Microbiol. 11 (2011) 13.
[11] T. Romantsov, J.M. Wood, Contributions of membrane lipids to bacterial cell homeostasis upon osmotic challenge, Biogenesis of Fatty Acids, Lipids and Membranes (Geiger, O., Ed.), Springer International Publishing, Cham, 2016, pp. 1–22.
[12] J.M. Wood, Perspective: challenges and opportunities for the study of cardiolipin, a key player in bacterial cell structure and function, Curr. Genet. 64 (2018) 795–798.
[13] D.C. Sévin, U. Sauer, Ubiquinone accumulation improves osmotic-stress tolerance in Escherichia coli, Nat. Chem. Biol. 10 (2014) 266–272.
[14] D.C. Sévin, J.N. Stählin, G.R. Pollak, A. Kuehne, U. Sauer, Global metabolic responses to salt stress in fifteen species, PLoS One 11 (2016) e0148888.
[15] C.F. Clarke, A.C. Rowat, J.W. Gober, Is CoQ a membrane stabilizer? Nat. Chem. Biol. 10 (2014) 242–243.
[16] L. Ernster, G. Dallner, Biochemical, physiological and medical aspects of ubiquinone function, Biochim. Biophys. Acta (BBA) - Mol. Basis Dis. 1271 (1995) 195–204.
[17] H. Saito, W. Shinoda, Cholesterol effect on water permeability through DPPC and PSM lipid bilayers: a molecular dynamics study, J. Phys. Chem. B 115 (2011) 15241–15250.
[18] W. Shinoda, Permeability across lipid membranes, Biochim. Biophys. Acta Biomembr. 1858 (2016) 2254–2265.
[19] B.B. Issack, G.H. Peslherbe, Effects of cholesterol on the thermodynamics and kinetics of passive transport of water through lipid membranes, J. Phys. Chem. B 119 (2015) 9391–9400.
[20] V. Agmo Hernández, E.K. Eriksson, K. Edwards, Ubiquinone-10 alters mechanical properties and increases stability of phospholipid membranes, Biochim. Biophys. Acta Biomembr. 1848 (2015) 2233–2243.
[21] E.K. Eriksson, V. Agmo Hernandez, K. Edwards, Effect of ubiquinone-10 on the stability of biomimetic membranes of relevance for the inner mitochondrial membrane, Biochim. Biophys. Acta 1860 (2018) 1205–1215.
[22] R.P. Rand, S. Sengupta, Cardiolipin forms hexagonal structures with divalent cations, Biochim. Biophys. Acta Biomembr. 255 (1972) 484–492.
[23] G.L. Powell, D. Marsh, Polymorphic phase-behavior of cardiolipin derivatives studied by p-31 nmr and x-ray-diffraction, Biochemistry. 24 (1985) 2902–2908.
[24] B. Kollmitzer, P. Heftberger, M. Rappolt, G. Pabst, Monolayer spontaneous curvature of raft-forming membrane lipids, Soft Matter 9 (2013) 10877–10884.
[25] T. Pilizota, Joshua W. Shaevitz, Plasmolysis and cell shape depend on solute outer-membrane permeability during hyperosmotic shock in E. coli, Biophys. J. 104 (2013) 2733–2742.
[26] V. Agmo Hernández, G. Karlsson, K. Edwards, Intrinsic heterogeneity in liposome suspensions caused by the dynamic spontaneous formation of hydrophobic active sites in lipid membranes, Langmuir. 27 (2011) 4873–4883.
[27] J.V. Paraskova, E. Rydin, P.J.R. Sjöberg, Extraction and quantification of phosphorus derived from DNA and lipids in environmental samples, Talanta. 115 (2013) 336–341.
[28] A. Kroger, Determination of contents and redox states of ubiquinone and menaquinone, Methods Enzymol. 53 (1978) 579–591.
[29] R.D. Kaiser, E. London, Location of diphenylhexatriene (DPH) and its derivatives within membranes: comparison of different fluorescence quenching analyses of membrane depth, Biochemistry. 37 (1998) 8180–8190.
[30] P.Y. Chen, D. Pearce, A.S. Verkman, Membrane water and solute permeability determined quantitatively by self-quenching of an entrapped fluorophore, Biochemistry. 27 (1988) 5713–5718.
[31] M.B. Lande, J.M. Donovan, M.L. Zeidel, The relationship between membrane fluidity and permeabilities to water, solutes, ammonia, and protons, J. Gen. Physiol. 106 (1995) 67–84.
[32] J.C. Mathai, S. Tristram-Nagle, J.F. Nagle, M.L. Zeidel, Structural determinants of water permeability through the lipid membrane, J. Gen. Physiol. 131 (2008) 69–76.
[33] W. Rawicz, B.A. Smith, T.J. McIntosh, S.A. Simon, E. Evans, Elasticity, strength, and water permeability of bilayers that contain raft microdomain-forming lipids, Biophys. J. 94 (2008) 4725–4736.
[34] M. Almgren, K. Edwards, G. Karlsson, Cryo transmission electron microscopy of liposomes and related structures, Colloids Surf. A Physicochem. Eng. Asp. 174 (2000) 3–21.
[35] S. Morein, A.S. Andersson, L. Rilfors, G. Lindblom, Wild-type Escherichia coli cells regulate the membrane lipid composition in a “window” between gel and non-lamellar structures, J. Biol. Chem. 271 (1996) 6801–6809.
[36] Y.Y. Chang, J.E. Cronan, Membrane cyclopropane fatty acid content is a major factor in acid resistance of Escherichia coli, Mol. Microbiol. 33 (1999) 249–259.
[37] M.A. Casadei, P. Manas, G. Niven, E. Needs, B.M. Mackey, Role of membrane fluidity in pressure resistance of Escherichia coli NCTC 8164, Appl. Environ. Microbiol. 68 (2002) 5965–5972.
[38] H. Hara, A. Hyono, S. Kuriyama, I. Yano, M. Masui, Electron-spin-resonance studies on the membrane-properties of a moderately halophilic bacterium. 2. Effect of extreme growth-conditions on liposome properties, J. Biochem. 88 (1980) 1275–1282.
[39] D. Poger, A.E. Mark, A ring to rule them all: the effect of cyclopropane fatty acids on the fluidity of lipid bilayers, J. Phys. Chem. B 119 (2015) 5487–5495.
[40] P. Wessman, K. Edwards, D. Mahlin, Structural effects caused by spray- and freeze-drying of liposomes and bilayer disks, J. Pharm. Sci. 99 (2010) 2032–2048.
[41] E. Mileykovskaya, W. Dowhan, Cardiolipin membrane domains in prokaryotes and eukaryotes, Biochim. Biophys. Acta Biomembr. 1788 (2009) 2084–2091.
[42] K.C. Huang, R. Mukhopadhyay, N.S. Wingreen, PLoS Comput. Biol. 2 (2006).
[43] R. Mukhopadhyay, K.C. Huang, N.S. Wingreen, Lipid localization in bacterial cells through curvature-mediated microphase separation, Biophys. J. 95 (2008) 1034–1049.
[44] N. Kučerka, S. Tristram-Nagle, J. Nagle, Structure of fully hydrated fluid phase lipid bilayers with monounsaturated chains, J. Membr. Biol. 208 (2006) 193–202.
[45] J. Pan, S. Tristram-Nagle, J.F. Nagle, Effect of cholesterol on structural and mechanical properties of membranes depends on lipid chain saturation, Phys. Rev. E 80 (2009) 021931.
[46] J. Hoyo, E. Guaus, G. Oncins, J. Torrent-Burgues, F. Sanz, Incorporation of ubiquinone in supported lipid bilayers on ITO, J. Phys. Chem. B 117 (2013) 7498–7506.
[47] J. Hoyo, E. Guaus, J. Torrent-Burgués, Tuning ubiquinone position in biomimetic monolayer membranes, Eur. Phys. J. E Soft Matter 40 (2017) 62.